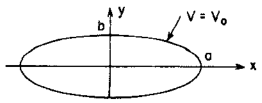

Fig. 2. Elliptic cross-section strip.

Hence

$$A\cosh V_0 = a \quad A\sinh V_0 = b$$

giving

$$\tanh V_0 = b/a. \tag{15}$$

If the ellipse degenerates into an infinitely thin strip, then $b = 0$ and $V_0 = 0$. For nonzero thin strips, b/a will be small, as will V_0, and we shall be concerned with very small, but nonzero, values of V_0.

The element $ds = [(dx)^2 + (dy)^2]^{1/2} = A dU[\cosh^2 V_0 - \sin^2 U]^{1/2}$ from (13). Hence the loss associated with the ellipse is proportional to

$$P_3 = \int_0^{2\pi} \frac{dU}{ds} dU = \frac{4}{A}\int_0^{\pi/2} \frac{dU}{\left[\cosh^2 V_0 - \sin^2 U\right]^{1/2}}$$

$$= \frac{4}{a} K(1/\cosh V_0) \tag{16}$$

where K is the complete elliptic integral of the first kind. For V_0 small the modulus is close to unity, and (16) has the expansion

$$P_3 = \frac{4}{a}\log(4\coth V_0) + O(V_0^2) \approx \frac{4}{a}\log(4a/b). \tag{17}$$

For an infinitely thin strip, $V_0 \to 0$, $x \to a\sin U$ and the losses are given by

$$P_4 = 4\int_0^{a-d}\left(\frac{dU}{dx}\right)^2 dx = 4\int_0^{a-d}\frac{dx}{a^2 - x^2} \approx \frac{2}{a}\log\frac{2a}{d} \tag{18}$$

for small d.

Comparing with (17) gives

$$d = b^2/8a = R/8 \tag{19}$$

where $R = b^2/a$ is the radius of curvature at the apex. Again, this is a "local" result in that it depends only on geometrical parameters close to the edge. Because the width of an ellipse near its apex is quite ill-defined, it is not possible to relate this result directly to an equivalent strip thickness.

V. Conclusions

The method of halting the loss integration a determinate distance just short of an edge enables loss perturbation calculations to be made with fields calculated for structures with infinitely thin strips or diaphragms. This should simplify such calculations considerably. The method encompasses a finite strip thickness with either a flat or rounded edge. In fact, the transformation of Section III would, if pursued to a potential surface $V_0 \neq 0$, be able to handle a variety of combinations of rounding and thickness.

References

[1] J. D. Cockroft, "Skin effect in rectangular conductors at high frequencies," *Proc. Roy. Soc (London) Ser. A*, vol. 122, pp. 533–542, 1929.
[2] H. Kaden, "Advances in microstrip theory," *Siemens Forsch. u Entwickl. Ber.*, vol. 3, no. 2, pp. 115–124, 1974.
[3] A. I. Nosich and V. P. Shestopalov, "Ohmic losses in transmission lines with thin conductors," *Sov. Phys. Dokl.*, vol. 25, pp. 127–128, Feb. 1980.
[4] H. A Wheeler, "Formulas for the skin effect," *Proc. IRE*, vol. 30, pp. 412–424, 1942.

A Technique for the Design of Microwave Transistor Oscillators

K. L. KOTZEBUE

Abstract —**A technique for the design of microwave transistor oscillators is presented in which measurements made on an experimentally optimized amplifier are used to calculate six basis oscillator circuits which yield maximum power output. The procedure has been experimentally verified by the construction of a silicon bipolar transistor test oscillator at 1 GHz.**

I. Introduction

A microwave transistor power amplifier is often easier to optimize experimentally than the corresponding microwave transistor oscillator. A transistor power amplifier is easily optimized because, at a given frequency and operating point, only two parameters need be varied: the input RF drive level, and the output load impedance (assuming that harmonic impedance terminations are not of first-order importance). Once these parameters are experimentally optimized, the design is completed by measuring the input impedance and constructing an input matching network. In the case of the transistor oscillator, however, there are a multitude of possible oscillator configurations, each more difficult to experimentally optimize for maximum power output than an amplifier. It is more difficult to experimentally optimize an oscillator for maximum power output because of the relatively large number of interacting circuit elements which must be varied, while maintaining a condition of oscillation. But since we know that a transistor operates under the same set of RF voltages and currents when delivering its maximum added power as an amplifier as it does when delivering its maximum output power as an oscillator, it should be possible to take information obtained from an easily optimized power amplifier and use this information to calculate optimum oscillator configurations. In this paper, such a design procedure is presented.

II. Design Procedure

The first step in the procedure is to experimentally optimize the large-signal performance of the transistor by varying the load impedance and RF drive level until the transistor's added power has been maximized. The load may be varied in the conventional fashion using stub tuners, etc., or the load may be synthesized by injecting a second signal into the output port in the manner reported by Takayama [1]. The incident and reflected waves a_1, b_1, a_2, and b_2, as shown in Fig. 1, can be measured on a network analyzer setup, and the added power computed from (1)

$$\text{Power} = |b_2|^2\left\{1 - \frac{1}{|S'_{22}|^2} - \frac{1 - |S'_{11}|^2}{|S'_{21}|^2}\right\} \tag{1}$$

where

$$S'_{11} \equiv \frac{b_1}{a_1}$$

$$S'_{22} \equiv \frac{b_2}{a_2}$$

$$S'_{21} \equiv \frac{b_2}{a_1}.$$

0018-9480/84/0700-0719$01.00

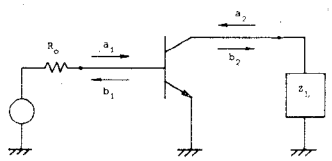

Fig. 1. Schematic representation of the transistor amplifier to be experimentally optimized.

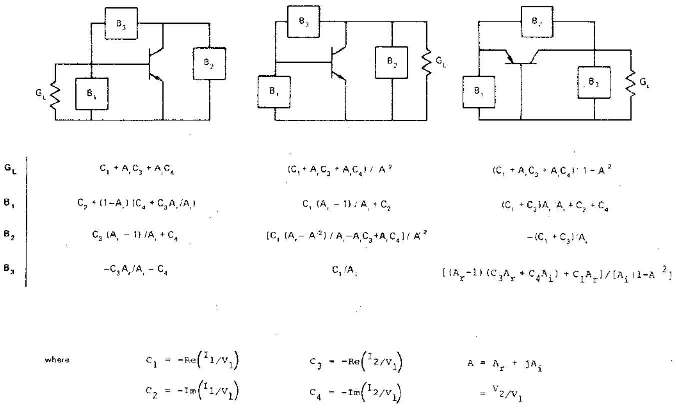

Fig. 2. Design equations for three-shunt oscillator topologies.

Using the three measured quantities S'_{11}, S'_{21}, and S'_{22}, it is then possible to calculate the needed ratios of terminal voltages and currents of the transistor by (2)

$$\frac{V_2}{V_1}=\frac{S'_{21}\left(\frac{1}{S'_{22}}+1\right)}{1+S'_{11}}$$

$$\frac{I_2}{I_1}=\frac{S'_{21}\left(\frac{1}{S'_{22}}-1\right)}{1-S'_{11}}$$

$$\frac{V_1}{I_1}=R_0\frac{1+S'_{11}}{1-S'_{11}}$$

$$\frac{V_2}{I_1}=R_0\frac{S'_{21}\left(1+\frac{1}{S'_{22}}\right)}{1-S'_{11}}$$

$$\frac{I_2}{V_1}=\frac{S'_{21}\left(\frac{1}{S'_{22}}-1\right)}{R_0\left(1+S'_{11}\right)}. \quad (2)$$

V_1 and I_1 are the transistor input port voltage and current, v_2 and I_2 are the transistor output port voltage and current, and R_0 is the characteristic impedance (assumed real) of the measuring system. These ratios rates are then used as indicated in Figs. 2 and 3 to obtain the values of all elements of six basic oscillator configurations; three of shunt topology and three of series topology. The equations in Figs. 2 and 3 are modified and corrected versions of those presented in [2] and employed by Johnson [3].

III. Experimental Results

This design procedure was tested using a NEC silicon bipolar transistor, NE73435, measured at 1 GHz. At a bias point of $V_{CE}=8$ V and $I_C=8$ mA, the maximum added power was

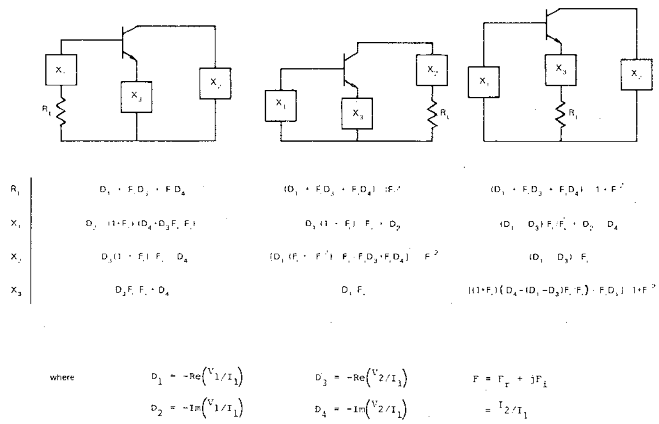

Fig. 3. Design equations for three-series oscillator topologies.

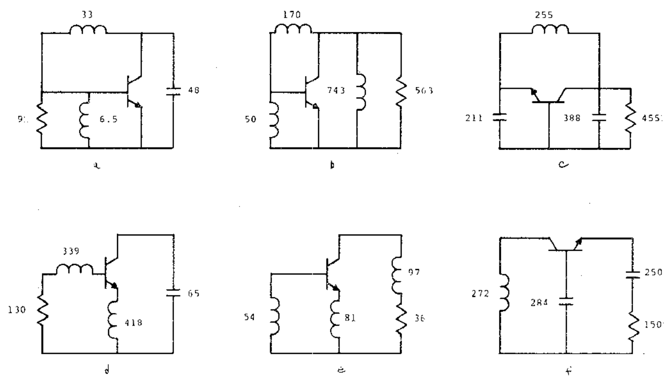

Fig. 4. Six computed oscillator configurations based on an experimentally optimized bipolar junction transistor at 1 GHz.

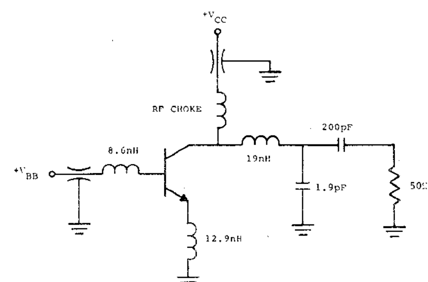

Fig. 5. Circuit diagram of a 1-GHz test oscillator.

measured to be 26 mW, with

$$S'_{11}=0.29\angle 132^\circ$$
$$S'_{21}=3.8\angle 33^*$$
$$S'_{22}=1.2\angle -37^\circ.$$

(In the notation used here, passive output loads correspond to $|S'_{22}|>1$.)

The oscillator configurations calculated from these measurements are shown in Fig. 4. It is interesting to note the wide range of circuit element values that are used in the various oscillator configurations; for example, the output resistive load varies from a high value of 563 to a low of 9 Ω. This gives the designer freedom to select a topology which is easiest to implement, while ensuring that the power output will be maximum. The configuration selected for implementation in this study was that of Fig.

4(e). The use of a simple L-section matching network at the output resulted in the circuit configuration of Fig. 5. This oscillator was constructed and yielded a stable oscillation at 1.03 GHz with a measured power output of 23 mW (36-percent efficiency), which is in good agreement with the predicted performance.

IV. Conclusion

In the design procedure presented here, no modeling or characterization of the transistor is required. Instead, a simple experimental amplifier optimization yields results which can be directly utilized in the calculation of six basic oscillator topologies, each delivering the same power. This procedure should be applicable to any two-port active device, provided that the effects of harmonic terminations are not of first-order importance, which is almost always the case with bipolar transistor and FET designs at microwave frequencies [4].

References

[1] Y. Takayama, "A new load-pull characterization method for microwave power transistors," in *1976 IEEE MTT-S Symp. Dig. of Papers*, pp. 218–220.

[2] K. L. Kotzebue and W. J. Parrish, "The use of large-signal S-parameters in microwave oscillator design," in *Proc. 1975 IEEE Int. Symp. on Circuits and Syst.*, Apr. 1975.

[3] K. Johnson, "Large-signal GaAs MESFET oscillator design," *IEEE Trans. Microwave Theory Tech.*, vol. MTT-27, pp. 217–227, Mar. 1979.

[4] R. J. Gilmore and F. J. Rosenbaum, "GaAs MESFET oscillator design using large-signal S-parameters," in *1983 IEEE MTT-S Symp. Dig. of Papers*, pp. 279–281.

Microwave Helix Waveguide Absorption Cell for Passive Frequency Standard

JEAN-CLAUDE MOLLIER AND MICHELLE VALENTIN

***Abstract*—A new closed absorption cell, which has been developed for a passive frequency standard, is described. This cell is made from a cylindrical quartz tube with copper wire wound around it. For the limiting case of the zero pitch helix, Maxwell's equations are graphically solved, which show that the cell is operating like a monomode waveguide at 23.8 GHz, the frequency of interest, and can be used from 10 to 100 GHz with few modifications.**

***Indexing Terms*—Microwave absorbtion cell, Helix waveguide, Mode filter, Passive frequency standard.**

A device was built using a stripline oscillator at 468 MHz, frequency-locked to the 3–3 ammonia line after a one-step frequency multiplication [1]. In order to ensure the stability of the absorption signal over a long period of time, with low-pressure gas (from 0.7 to 1 Pa) and low-excitation power (1 mW), a carefully designed cell is needed: the walls must be made from inert material in order to avoid reaction with ammonia gas and rapid disappearance of the signal. The cell must behave as a nonresonant structure, with small vibrations sensitivity and reduced losses. After testing many types of absorption cells, a unique closed cell has been developed, which behaves like a monomode helix waveguide [2],[3].

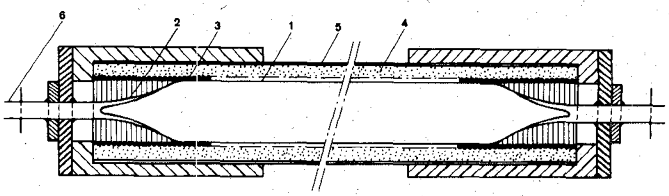

Fig. 1. Longitudinal cutaway of the helix cell. 1—sealed quartz tube. 2—transitions: guide-emitter, guide-detector. 3—closely wound turns of insulated copper. 4—flexible carbon polyurethane foam. 5—copper cylinder. 6—waveguide.

A longitudinal cutaway is shown in Fig. 1. The cell is made from a cylindrical fused-quartz tube, whose ends are tapered to a point providing a smooth transition and a degree of matching with the K-band metallic waveguides. The tube has inner and outer diameters of 23 and 25 mm, respectively. Insulated copper wire is wound on the tube so as to make a helix of very small pitch (closely wound turns). In order to reduce mode conversion-reconversion effects and external radiation, the helix is surrounded by a lossy medium (flexible carbon-loaded polyurethane foam) and by a coaxial copper shield which makes the device insensitive to shocks. The helix cell is inserted between two circular horns which are connected, through K-band rectangular waveguides, the one to the multiplier output, the other one to a matched detector.

The round wire helix covered by the lossy jacket provides a low attenuation of the TE_{on} propagation mode in cylindrical waveguide and a very large attenuation for all other modes: the real part of the propagation constant is of the order of 2×10^{-2} dB/m for the TE_{01} mode and is varying from 10 to 200 dB/m for the first hybrid modes.

This filtering efficiency has been verified experimentally by studying the resonant modes of resonators realized from a section of oversized helix waveguide and from a section of circular metallic pipe with the same length and diameter [4]. The helix waveguide with dielectric coating is effectively a good mode filter.

The circular metallic guide with inner dielectric coating is an asymptotic case of the type of guide under consideration for the propagation of TE_{on} modes. Special attention is then given here to the limiting case of a zero pitch helix surrounding the quartz tube. Maxwell's equations are solved by following the procedure set up by Stratton [5] for the classical cylindrical waveguide boundary problem. The fields confined into the tube are found by assuming that the helical sheath is perfectly conducting in the transverse direction and does not conduct in the longitudinal one. The application of boundary conditions for E and H fields gives the two following equations:

$$\frac{J_1(b/ax_1)}{x_1 J_0(b/ax_1)} = \frac{1}{x_2}\cdot\frac{J_1(x_2)Y_1(b/ax_2)-J_1(b/ax_2)Y_1(x_2)}{J_1(x_2)Y_0(b/ax_2)-J_0(b/ax_2)Y_1(x_2)} \tag{1}$$

$$x_2^2 - x_1^2 = \left(\frac{2\pi a}{\lambda_0}\right)^2\cdot(\epsilon_r - 1) \tag{2}$$

$$x_1^2 = a^2(\omega^2\mu_0\epsilon_0 - \beta^2)$$

$$x_2^2 = a^2(\omega^2\mu_0\epsilon_0\epsilon_r - \beta^2) \tag{3}$$

Manuscript received July 7, 1983; revised January 16, 1983.

J.-C. Mollier is with the Laboratoire de Communications Optiques et Micro-ondes, Université de Limoges, 87060 Limoges Cedex, France.

M. Valentin is with the Laboratoire de Physique et Metrologie des Oscillateurs du C.N.R.S., assorié à l'Université de Franche-Comté-Besançon, 25000 Besançon, France.

0018-9480/84/0700-0721$01.00 ©1984 IEEE